

## Part B: Full Proposal

### Simulating Multi-component Aerosol Filters via Geometrical Modeling and Volumetric Imaging

H. V. Tafreshi (PI), B. Maze (Co-PI) and B. Pourdeyhimi (Co-PI)  
NC State University

#### Proposal Summary

While there are numerous analytical expressions available for predicting the pressure drop and collection efficiency of the single-component filters (filters with a single fiber diameter) made up of circular fibers, there are practically no such relations for multi-component filters (filters with different fiber diameters). In this proposal, pressure drop per unit thickness and collection efficiency of multi-component filters and made up of circular and non-circular fibers will be calculated via numerical simulation. Digital Volumetric Imaging (DVI) technique will be used to reconstruct the real 3-D geometries of air filters. Real and modeled 3-D geometries will be used in the simulation for comparison and benchmarking, and therefore, drawing solid conclusions.

GeoDict a Computational Fluid Dynamics (CFD) developed by ITWM, Germany will be used in this study along with the CFD code from Fluent Inc to simulate aerosol flow through 3-D filter structures. This study completes our on-going NCRC project # 04-70 entitled "Filtration by Micro and Nanofiber Filters: Simulation and Experiment" which ends in August 2007. Specific targets of the current proposal are the followings:

- Obtain expressions for predicting pressure drop and collection efficiency of multi-component filters
- Study the influence of the fiber cross-section on the filter's pressure drop and collection efficiency
- Compare the simulations of modeled filters with those performed on real structures obtained via Digital Volumetric Imaging (DVI)

#### Specific Objective:

Obtain pressure drop and collection efficiency expressions for multi-component filters, establish influence of fiber cross section, and compare simulations of modeled filters with those performed on structures obtained via DVI.

#### 1-Introduction

The pressure drop and collection efficiency of fibrous filters have been studied for many years and numerous analytical, numerical and empirical correlations are available for such media. In almost all these models, a filter is assumed to be made up of fibers with a unimodal fiber diameter distribution (from now on called mono-component filters) and with circular cross-sections. Moreover, the existing models assume the filter to

consist of fibers arranged on a regular lattice which is obviously not accurate. A great portion of the fibrous filters is made up of blends of coarse and fine fibers with widely different average diameters and cross-sectional shape. This is often the case where mechanical strength and filtration efficiency are both important. The fine fibers contribute to the high filtration efficiency (high collection efficiency for a given pressure drop) while the coarser fibers contribute to the medium's rigidity. The fibers may be intimately blended in the case of short fibers like in carded, air-laid, or wet-laid fiberwebs or layered in the case of melt-spun media such as melt-blown and/or spunbonded webs. Despite their importance, no simple expressions exist for calculating the pressure drop of filters with bimodal fiber diameters (from now on called bi-component filters) or multimodal fiber diameters (from now on called multi-component filters). This is probably because of the presence of too many independent but coupled variables which contribute greatly to the complexity of such calculations. The current proposal is aimed at improving our understanding of the influence of different variables on the permeability and collection efficiency of multi-component filters. We will pay special attention to the filters made up of fibers with noncircular cross-sections.

## 2-Background Information

In almost all existing models, the pressure drop of mono-component filters is estimated via solving the air flow governing equations through the media modeled by a structured array of fibers in two or three dimensional space. All these models present the pressure drop per unit thickness of mono-component filter as:

$$\frac{\Delta p}{t} = f(\phi) \frac{\eta V}{r^2}$$

For a constant fluid viscosity,  $\eta$ , filter face velocity,  $V$ , and fiber radius,  $r$ , pressure drop per unit thickness becomes a function of the medium's Solid Volume Fraction (SVF),  $\phi$ , alone.

The problem is much more complicated for the case of multi-component filters. In the case of bi-component filters, for instance, we assumed the pressure drop per unit thickness to have the following form [1]:

$$\frac{\Delta p}{t} = f(\phi, d_c, d_f, R_{cf}, F_c)$$

where  $d_c$  and  $d_f$  are diameters of the coarse and fine fibers,  $R_{cf} = d_c / d_f$  is the diameter ratio of coarse fiber to fine fiber, and  $F_c$  is the number fraction of the coarse fibers (the number of coarse fibers divided by the total number of fibers in the medium). Obviously,  $F_f = 1 - F_c$ , where  $F_f$  is the number fraction of the fine fibers. We have obtained an equivalent diameter,  $d_{eq}^*$  as a function of  $R_{cf}$ , and  $F_c$  in a 2-D model. This equivalent diameter when used in the existing mono-component 2-D models of fibrous

filters showed excellent agreement with the pressure drop results of bi-component filters [1]. In the current proposal we plan to extend this previous work to more realistic 3-D geometries.

Similar to the above-mentioned pressure drop calculation, there are available models for predicting the filtration efficiency of mono-component filters. However, there is no model for bi-component or multi-component filters. In single fiber theory, collection efficiency of a mono-component filter can be obtained by the single fiber efficiency [2]:

$$E = 1 - \exp\left(\frac{-4\alpha E_{\Sigma} t}{\pi d_f}\right)$$

in which  $t$  is the thickness of the filter and  $d_f$  is the fiber diameter.

Again, note that such an equation is not valid for a bi-component or multi-component filter.

## 2.1-Single Fiber Theory

Interception, inertial impaction and Brownian diffusion are three most important capture mechanisms. The mechanical single fiber efficiencies can be calculated as follows.

$$E_{\Sigma} = 1 - (1 - E_R)(1 - E_I)(1 - E_d)$$

where Single Fiber Efficiency (SFE) due to the interception  $E_R$ , is given as [3, 4, 5]:

$$E_R = \frac{1+R}{2Ku} \left[ 2\ln(1+R) - 1 + \alpha + \left(\frac{1}{1+R}\right)^2 \left(1 - \frac{\alpha}{2}\right) - \frac{\alpha}{2}(1+R)^2 \right]$$

in which  $Ku = -0.5\ln\alpha - 0.75 + \alpha - 0.25\alpha^2$  is the Kuwabara's hydrodynamic coefficient and  $R = d_p / d_f$  is the particle-to-fiber diameter ratio where  $d_p$  is the particle diameter.

SFE due to inertial impaction  $E_I$ , is given by [4,5]:

$$E_I = \frac{(Stk)J}{2Ku^2}$$

where  $J = (29.6 - 28\alpha^{0.62})R^2 - 27.5R^{2.8}$  for  $R < 0.4$  and  $Stk = \rho_p d_p^2 C_c V / 18\eta d_f$  is the Stokes number, defined as the ratio of particle stopping distance to the fiber diameter (Hinds 1999). Here  $\rho_p$ ,  $\eta$ , and  $V$  are particle density, air viscosity, and the flow velocity, respectively.

$C_c = 1 + Kn_p (1.257 + 0.4e^{-1.1/Kn_p})$  is an empirical correction factor called Cunningham slip correction factor and is used only for nanoparticles where the no slip condition on the wall is invalid [1,5]. Here  $Kn_p = 2\lambda/d_p$  is the particle Knudsen number and  $\lambda = \bar{R}T / \sqrt{2}N_a\pi d_m^2 p$  is the mean free path of the air molecules, where  $d_m = 3.7 \times 10^{-10}$  m is the collision diameter of the air molecules.  $p$  and  $T$  are the air pressure temperature, respectively.  $N_a$  and  $\bar{R}$  are the Avogadro number and the universal gas constant, respectively. The smaller the particle, the greater is the slip correction factor. Note that the higher the slip, the weaker is the coupling between the particles and the carrier gas and therefore, the trajectory of a particle is expected to have a greater deviation from its original streamline. Using the Kuwabara cell model, Lee and Liu [6] obtained an expression for the SFE of Brownian diffusion,  $E_d$ :

$$E_d = 2.6 \left( \frac{1-\alpha}{Ku} \right)^{1/3} Pe^{-2/3}$$

in which  $Pe = Vd_f/D$  is the Peclet number,  $D = \sigma C_c T / 3\pi\eta d_p$  is the diffusion coefficient, and,  $\sigma = 1.38 \times 10^{-23} \text{ m}^2 \text{ kg s}^{-2} \text{ K}^{-1}$  is the Boltzmann constant. We will use single fiber theory for deriving expressions for calculating bi-component filter efficiency.

### 3-Virtual Filter Structure

#### 3.1-Modeled Structures

Fiber orientation is an important structural characteristic. Clearly, the properties of a nonwoven filter depend on the nature of the component fibers as well as the way in which the fibers are arranged. The fiber orientation is an important structural feature that will control the behavior and the anisotropy of the structure. The same is true for fiber diameter and the fraction of each fiber type in a multi-component filter. GeoDict allows the user to have control on the fiber-web properties. This includes but is not limited to:

- Desired SVF (or porosity),
- Single or multi-component filters,
- Fibers with different cross-sections such as Circular, Elliptical, Trilobal, Rosetta
- Fiber orientation distribution in 2 and 3 dimensional space
- Overlapping and non-overlapping fibers with a control on the fiber-to-fiber spacing

We plan to use GeoDict for generating variety of multi-component filters with fibers having different cross-sections. The picture below shows a mono-component fiber-web with fibers having trilobal cross-sections.

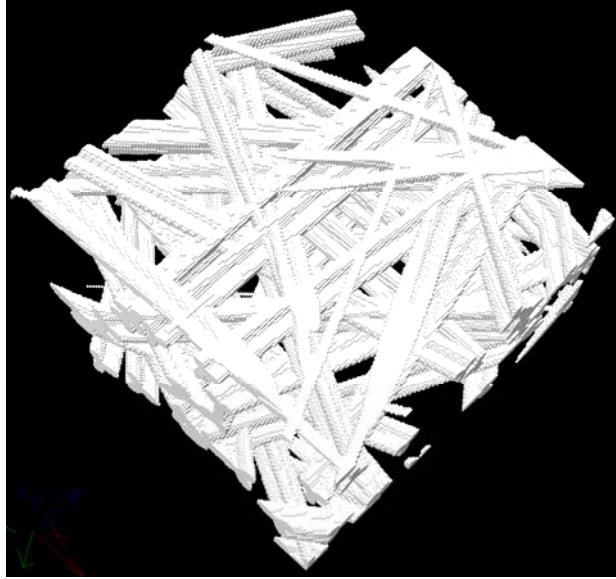


**Figure 1:** An example of a mono-component fiber-web with fibers having trilobal cross-sections.

The picture below is an example of an intimate blend of circular and trilobal fibers with equal mass fractions in a bi-component fiber web. These fiber-webs will be compared with those we generate using our in-house 3-D fiber-web generator for benchmarking both software programs [7].



**Figure 2:** An example of a bi-component fiber-web made up of fibers with circular (red) and trilobal (white) cross-sections. Both components have equal mass fractions.

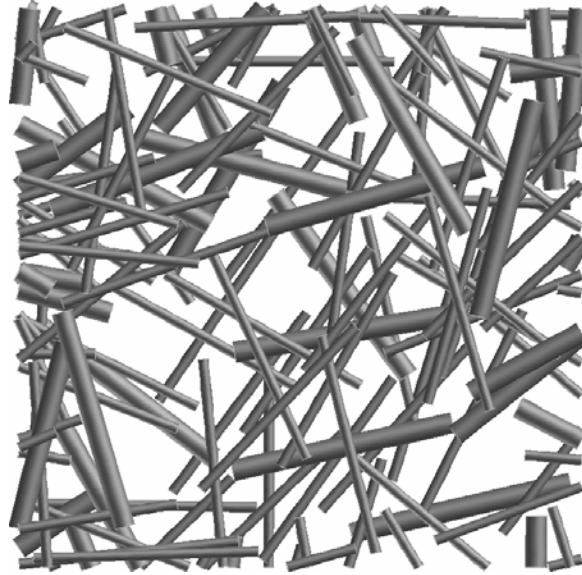


**Figure 3:** An example of a bi-component fiber-web made up of fibers with circular cross-sections.

### **3.2-Real Structures**

Apart from the “modeled” geometries that GeoDict can generate, it is also capable of constructing 3-D images obtained via Digital Volumetric Imaging (DVI). These 3-D images are then converted to 3-D physical geometries and used for flow simulation in GeoDict flow solvers. We plan to use GeoDict for simulating aerosol flow through real multi-component filters.

#### **3.2.1-Digital Volumetric Imaging (DVI)**

Here we propose using a digital volumetric imaging method which can reveal the real 3-D nature of the fibrous structures. The information obtained from DVI can be used to virtually construct the exact geometry of the media for fluid flow computations.

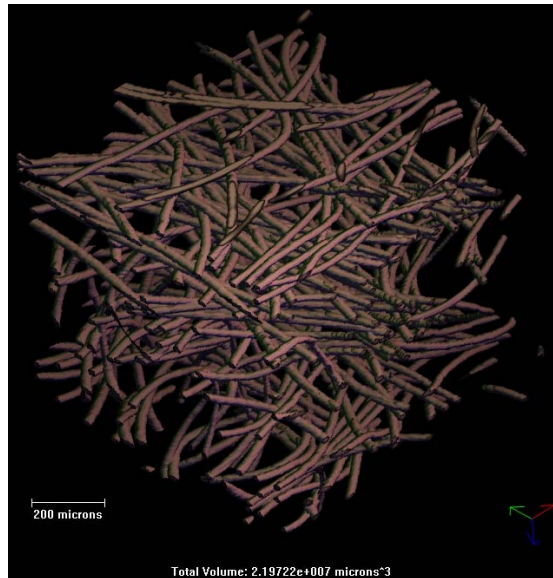


**Figure 4:** An example of a DVI image obtained from a hydroentangled fabric for illustration purposes only. We will obtain DVI images from aerosol filters for this research.

Conventional 3-D imaging methods depend on taking serial sections from a sample block and rendering these images to 3-D format. DVI is a fluorescent imaging technique. Samples are prepared by fluorescent dyeing of the fibers, dehydration, and embedding the samples in a polymer matrix. Image acquisition is performed by automated slicing of the polymer matrix and taking microscopic images. These serial images can be then volume-rendered to obtain high-fidelity 3-D images.

Figure 4 shows an example of DVI images. This image is taken from a hydroentangled fabric just for illustration purposes. We will use air filter media for DVI imaging in this proposal. Resolution of the images ranges from 0.44  $\mu\text{m}$  to 4.44  $\mu\text{m}$  depending upon size of the sample.

#### **4-Modeling Strategy**

Depending on the available computational memory, 3-D structures will be generated and exported to GeoDict and Fluent codes for aerosol flow simulations. Different numerical algorithms, including but not limited to, those used in our previous works will be considered for these new simulations [5, 8, 9, 10]. Basically, Navier-Stokes equations will be solved for the air flow through the filters:

$$\frac{D\rho}{Dt} + \rho \nabla \cdot V = 0$$

$$\rho \frac{DV}{Dt} = -\nabla p - \eta \nabla \times (\nabla \times V) + 4/3 \eta \nabla (\nabla \cdot V)$$

$$\rho c_p \frac{DT}{Dt} = -\frac{Dp}{Dt} + k \nabla^2 T$$

Once the particle-free flow field is obtained, the airborne particulates, modeled by rigid spheres will be introduced into the solution domain. The rationale for this method is the dilution of the suspension, which leads to negligible perturbations of the continuum field by the presence of the particulate phase. Particle trajectories are then tracked via the Lagrangian method and their positions are monitored. In the Lagrangian method, the force balance on a particle is integrated to obtain the particle position in time. The dominant forces acting on the nanoparticles are drag force exerted by the flow and the Brownian force:

$$\frac{dv_{i_p}}{dt} = F_d (v_i - v_{i_p}) + F_{b_i}$$

where  $v_i$  and  $v_{i_p}$  are the field and particle velocity in the  $x$ ,  $y$ , or  $z$  direction.  $F_d$  and  $F_{b_i}$  are amplitudes of the drag (for  $Re_p = \frac{\rho V d_p}{\eta} < 1$ ) and Brownian force given as:

$$F_d = \frac{18\eta}{d_p^2 \rho_p C_c}$$

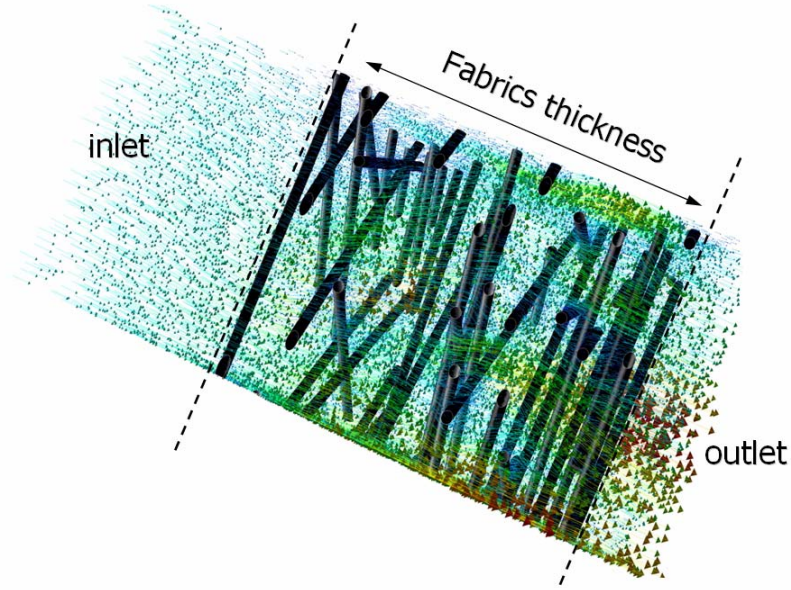
and

$$F_{b_i} = \frac{18\mu\zeta_i}{d_p^2 \rho_p C_c} \sqrt{\frac{2\nu}{\Delta t Sc}}$$

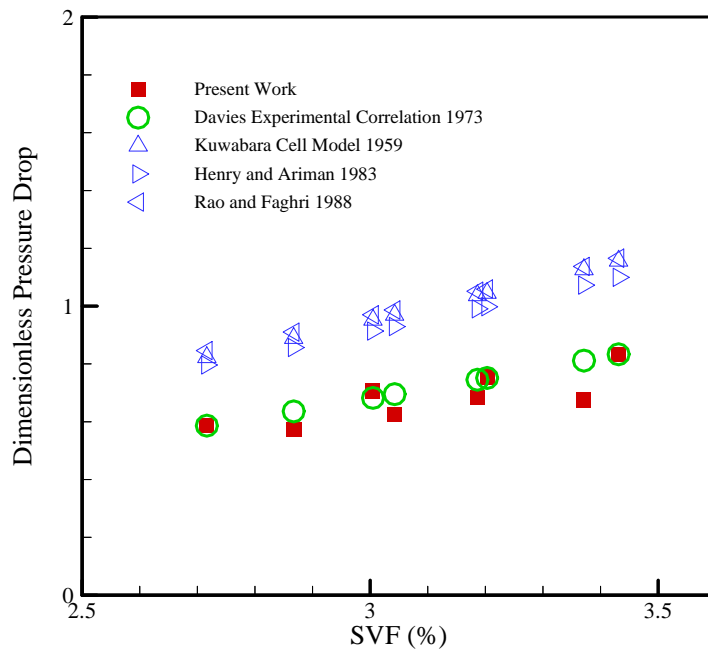
where  $Sc$  is the Schmidt number defined as  $Sc = \frac{3\pi d_p \eta \nu}{C_c \sigma T}$ ,  $\zeta_i$  are zero-mean, unit-variance independent Gaussian random numbers [5].

Figure 5 shows an example of the air flow field inside a virtual air filter. The pressure drop across an ensemble of such filters is calculated and compared with experiment. An excellent agreement has been observed and reported in detail in our published work [5].

Nanoparticles are released in this flow domain and their trajectories are tracked to calculate the number of collisions with the fibers and so the particle filtration efficiency of the filter [5].



**Figure 5:** Velocity field shown with velocity vectors inside a 3-D virtual filter



**Figure 6:** Pressure drop calculation from our CFD simulations compared with other existing models and the empirical equation of Davies (1973). It can be seen that our model is the only one matching with experiment.

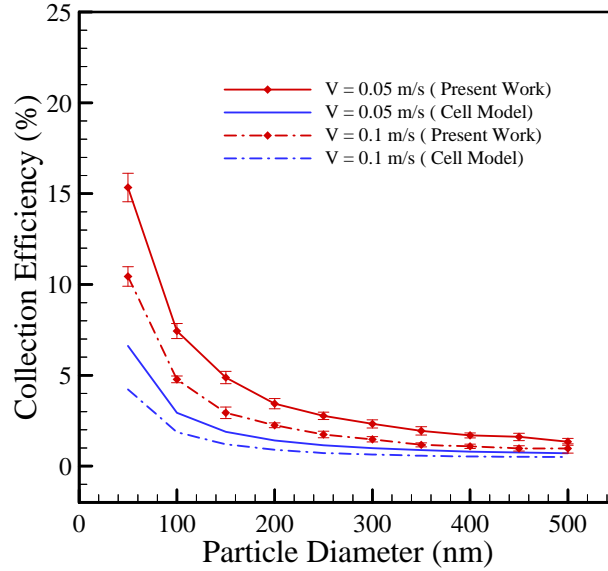


**Figure 7:** Collection efficiencies for two different face velocities of 0.1 and 0.05 m/s are shown. Kuwabara’s cell model predictions are also presented for comparison.

We plan to conduct similar computer simulations with GeoDict and take advantage of its unique capabilities. We will firstly benchmark GeoDict’s calculations by comparison with Fluent’s results and available expressions and then explore new possibilities. Figure 8 shows an example of particle deposition simulation via GeoDict software.

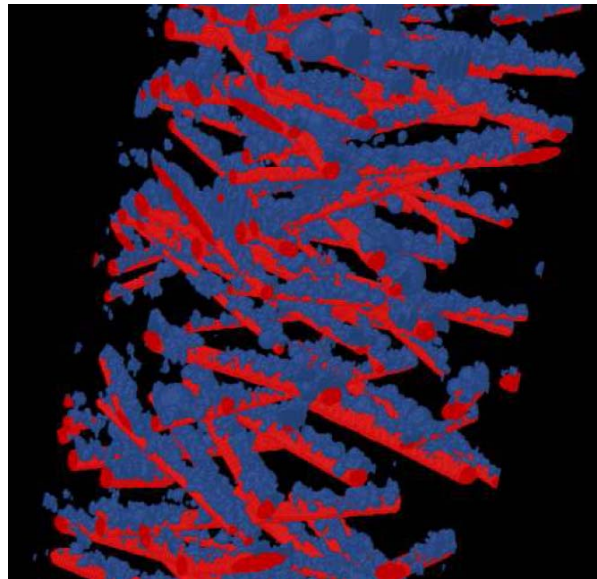


**Figure 8:** An example of particle deposition (blue) on the fiber surface (red).

We also plan to simulate real filter media both in GeoDicty and Fluent. 3-D real structures will be cut from the images like the one shown in Figure 4 and imported to

GeoDict and Fluent software for aerosol flow simulation. Figure 9 shows an example of such 3-D structures in Fluent code. The sample size is small as it is made for demonstration of the technique only.



**Figure 9:** An example of a real 3-D structure imported in Fluent code for illustration purposes. The sample is taken from Figure 4.

This way we take advantage of the capabilities of both CFD codes to better our understanding of bi-component and multi-component filters with and without circular fibers.

#### **Millstones:**

##### **1<sup>st</sup> year: Benchmarking modeled geometries**

Using DVI system, we will obtain 3-D structures of real filters (after measuring their filtration efficiency by TSI 3160) and simulate aerosol flow through them. The results of this study will be compared with that of flow through modeled geometries. We assess the accuracy of our modeling.

##### **2<sup>nd</sup> year: Multicomponent filters having fibers with circular cross-sections**

We will generate series of fibrous structures with different fiber components to establish a relation for between the blend ratios and filtration efficiency for each diameter ratios.

##### **3<sup>rd</sup> year: Multicomponent filters having fibers with noncircular cross-sections**

We will extend the above study to filters with noncircular fibers and draw overall conclusions to be used in product development.

## References:

1. S. Jaganathan, H. Vahedi Tafreshi, and B. Pourdeyhimi (under review) "On the Pressure Drop Prediction of Filter Media with Bimodal Fiber Diameter" *Powder Technology*
2. W. C. Hinds (1982) "Aerosol Technology: Properties, Behavior, and Measurement of Airborne Particles" Wiley, Cop. New York.
3. H. Yeh and B. Y. H. Liu (1974) "Aerosol Filtration by Fibrous Filters-I Theoretical" *J. Aerosol Sci.* 5, 191-204
4. R. C. Brown (1984) "A Many-fiber Model of Airflow through a Fibrous Filter" *J. Aerosol Sci.* 17, 4, 685-697
5. Q. Wang, B. Maze, H. Vahedi Tafreshi, and B. Pourdeyhimi (2006) "A Note on Permeability Simulation of Multifilament Woven Fabrics" *Chemical Engineering Science*, 61, 8085-8088
6. K. W. Lee and B.Y.H. Liu (1982) "Theoretical Study of Aerosol Filtration by Fibrous Filters" 1(2), 147-161
7. B. Pourdeyhimi, B. Maze, and H. Vahedi Tafreshi (2006) "Simulation and Analysis of Un-bonded Nonwoven Fibrous Structures" *Journal Engineered Fibers & Fabrics*, 1, 2
8. Q. Wang, B. Maze, H. Vahedi Tafreshi, and B. Pourdeyhimi (2006) "A Case Study of Simulating Submicron Aerosol Filtration via Spun-bonded Filter Media" *Chemical Engineering Science*, 61, 4871-4883 (2006)
9. S. Zobel, B. Maze, H. Vahedi Tafreshi, and B. Pourdeyhimi (under review) "Simulating Permeability of 3-D Calendered Fibrous Structures" *Chemical Engineering Science*
10. B. Maze, Q. Wang, H. Vahedi Tafreshi, and B. Pourdeyhimi (under review) "Unsteady-state Simulation of Nanoparticle Aerosol Filtration via Nanofiber Electrospun Filters at Reduced Pressures" *Journal of Aerosol Science*

## PROJECTED BUDGET

### Simulating Multi-component Aerosol Filters via Geometrical Modeling and Volumetric Imaging

**H. V. Tafreshi (PI), B. Maze (Co-PI) and B. Pourdeyhimi (Co-PI)**

NC State University

**Years Project Duration: 3**

Personnel Section	
PI (Faculty) Name	Summer Salary <sup>1</sup>
	\$/year
<b>H. V. Tafreshi</b> (0.5 month)	5,000.00
<b>B. Maze</b> (0.5 month)	5,000.00
Behnam Pourdeyhimi (0 month)	0.00
	\$/year
Graduate Students - 1	18,000.00
Other - Tuition	8,000.00
Fringe Benefits	4,483.00
<b>Total Personnel</b>	<b>42,483.00</b>
Travel	2,000.00
Supplies	4,000.00
	48,483.00
<b>Total Annual Direct Charges</b>	
<b>Total Annual Indirect Charges</b>	-0 <sup>-2</sup>
<b>Total Equipment Cost</b> (See note below) <sup>3</sup>	0,000.00
<b>Total Project Life Budget</b>	<b>145,449.00</b>

**Included in Equipment Cost above are following items over \$5,000 / item**

Brief Item Name	College or University	Amount - \$

- (1) Maximum of one month for one PI. Multiple PI proposals receive a proportion according to their participation level
- (2) NCRC projects are exempt from indirect costs.
- (3) All equipment will be returned to NCRC after the completion of the project.